Poly(A) tail degradation in human cells: ATF4 mRNA as a model for biphasic deadenylation

Béatrice Jolles, Olivier Jean-Jean*

Sorbonne Université, Institute of Biology Paris-Seine, IBPS, CNRS, Biological Adaptation and Ageing, B2A, F, 75005, Paris, France

ARTICLE INFO

ABSTRACT

Eukaryotic mRNA deadenylation is generally considered as a two-step process in which the PAN2–PAN3 complex initiates the poly(A) tail degradation while, in the second step, the CCR4-NOT complex completes deadenylation, leading to decapping and degradation of the mRNA body. However, the mechanism of the biphasic poly(A) tail deadenylation remains enigmatic in several points such as the timing of the switch between the two steps, the role of translation termination and the mRNAs population involved. Here, we have studied the deadenylation of endogenous mRNAs in human cells depleted in either PAN3 or translation termination factor eRF3. Among the mRNAs tested, we found that only the endogenous ATF4 mRNA meets the biphasic model for deadenylation and that eRF3 prevents the shortening of its poly(A) tail. For the other mRNAs, the poor effect of PAN3 depletion on their poly(A) tail shortening questions the mode of their deadenylation. It is possible that these mRNAs experience a single step deadenylation process. Alternatively, we propose that a very short initial deadenylation by PAN2-PAN3 is followed by a rapid transition to the second phase involving CCR4-NOT complex. These differences in the timing of the transition from one deadenylation step to the other could explain the difficulties encountered in the generalization of the biphasic deadenylation model.

© 2021 The Authors. Published by Elsevier B.V. This is an open access article under the CC BY-NC-ND license (http://creativecommons.org/licenses/by-nc-nd/4.0/).

1. Introduction

The 5-methylguanosine cap and the poly(A) tail both contribute to protect eukaryotic mRNAs against degradation. Deadenylation is the initial and rate-limiting step of the general mRNA decay pathway [1]. It is followed by either (i) the removal of the 5′ cap structure by one of the decapping enzymes, DCP1 or DCP2, and the 5′ to 3′ digestion of the mRNA body by the exonuclease XRN1, or (ii) the 3′ to 5' degradation of the mRNA body by the exosome-mediated pathway (reviewed in Refs. [2,3]).

In mammals, the mRNA poly(A) tail commonly has 200-250 adenosine residues. Two major mRNA deadenylation complexes, PAN2–PAN3 and the CCR4-NOT [4], have been involved in the 3′ to 5′ poly(A) tail degradation pathway [5]. The PAN2-PAN3 deadenylation complex is composed of a PAN2 molecule wrapped around an asymmetric homodimer of PAN3. To initiate deadenylation, the two PAN3 subunits recognize two poly(A)-bound PABP molecules allowing the RNase active site of PAN2 to remove the 3′ terminal A residues of mRNA poly(A) tail [6,7]. In human cells, the multisubunit CCR4-NOT complex is constituted by the association of 5 NOT proteins with two deadenylases, CCR4 (also named CNOT6) and CAF1 (also named CNOT7). TOB associates with the CCR4-NOT complex via interaction with CAF1 [8,9]. Using Tet-promoter driven transcriptional pulsing approach and a β-globin reporter gene, it has been assessed that the deadenylation of mRNAs is a biphasic process in which the PAN2–PAN3 complex first shortens the 3′ poly(A) tail to approximately 100 nt, before the process is completed by the CCR4-NOT complex which degrades the remaining poly(A) tail up to ~20 nt [5,10,11]. This second step proceeds in a less synchronous way than the PAN2–PAN3 deadenylation process and could be concomitant with the 5′-3′ decay of the mRNA body [5,10].

The Poly(A)-binding protein (PABP) has been shown to be a key actor in the deadenylation mechanism. Indeed, this major mRNA-interacting protein that covers the mRNA poly(A) tail (one PABP molecule interacts with ~27 adenosine residues) was first described to have a protective effect against mRNA degradation [12]. Afterwards, it has been established that poly(A) tail-bound PABPs play an active role in mRNA degradation by recruiting the deadenylation complexes through interaction between their MLLE domain and

---

proteins carrying a PAM2 motif (PABP-interacting motif 2) such as PAN3 [13] and TOB [11]. In addition to PAN3 and TOB, the eukaryotic release factor 3 (eRF3) which carries two overlapping PAM2 motifs, binds to the MLLE domain of PABP [14]. eRF3 is a small GTPase which associates with eukaryotic release factor 1 (eRF1) to terminate translation when a stop codon enters the A site of the ribosome. Several reports have demonstrated that the affinity of eRF3 for PABP is greater than that of PAN3 and TOB, possibly due to the presence of its two PAM2 motifs [14] and that termination and deadenylation complexes are exchanged on PABP in a translation-dependent manner [10]. The competition between eRF3 and deadenylation complexes for their interaction with PABP suggests that eRF3 has a protective effect against deadenylation. As a general scheme, it has been proposed that, upon translation termination, an eRF3 molecule bound to a poly(A) tail-associated PABP is recruited to the ribosome, allowing a deadenylase complex to bind to the PABP molecule now available for this new interaction [10,14]. This exchange would initiate poly(A) tail degradation. Previous works studying cytoplasmic poly(A) tail length either on reporter genes [1,15] or on a genome-wide scale [16—19] have shown that, in steady state conditions, the cytoplasmic poly (A) tail of translated mRNAs is highly heterogeneous in size, resulting from heterogeneous synthesis by poly(A)-polymerase in the nucleus and ongoing deadenylation. Thus, for a given mRNA, the average tail lengths is in the range of 50—100 adenosines, with only a small portion ranging up to 200-250 adenosines.

However, despite a great deal of advances in the knowledge of genome-wide poly(A) tail profiling, which has been afforded by the development of next generation sequencing methods [16—20], our knowledge on poly(A) tail degradation mechanism has not changed much [21]. Indeed, very little is known on the extend of the biphasic deadenylation process in mRNA decay and despite recent extensive work on the structure and activity of the deadenylation complexes [19,22], the relationship between deadenylation rate, mRNA stability and translation remains obscure [23]. Moreover, the role of eRF3 in biphasic deadenylation remains enigmatic suffering from the lack of endogenous cellular mRNA examples.

Ligase-Mediated Poly(A) test (LM-PAT) allows mRNA poly(A) tail length to be analysed in great details. In brief, LM-PAT consists of saturating the entire poly(A) tail after ligation of hybridized oligo(dT)$_{12-18}$ primers as well as a (dT)$_{12}$ − anchor primer at the 3′-most end of the poly(A) tail (Fig. 1). The ligated oligos serve as primer for a cDNA reaction and poly(A) tail length is determined by a PCR reaction using a forward gene-specific primer and the (dT)$_{12}$ − anchor primer as reverse primer. PCR forward primers are designed close to the 3′ end of the mRNA in order to obtain, after amplification, 250 to 500 base pairs long DNA fragments [24]. Since such assays proved to be effective for studying polyadenylation [25] or deadenylation of specific mRNAs like those engaged in translation [26], we wondered whether this method would allow to get additional information on the biphasic mechanism of mammalian mRNA deadenylation. Unlike Northern blot which analyses the whole mRNA molecule, LM-PAT specifically analyses mRNA 3′-end and information only reflect changes in poly(A) tail length.

Here, we explore the tail-length dynamics of endogenous mRNAs in the situation of either translation termination or PAN2-PAN3 deadenylase defects. We demonstrated that ATF4 (activating transcription factor 4) mRNA corresponds to an endogenous model for biphasic deadenylation, with PAN2-PAN3 complex involved in the first step of deadenylation and eRF3 affording a clear protection against deadenylation.

2. Materials and methods
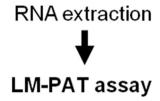
2.1. Cell culture and cell electroporation

The HCT116 cell line (ATCC CCL-247) was maintained in McCoy medium (Invitrogen) supplemented with 10% fetal calf serum, 1 mM sodium pyruvate, 100 μg/ml streptomycin and 100 units/ml penicillin at 37 °C under 5% CO2 atmosphere. HEK293 cells (ATCC CRL-1573) were cultured in Dulbecco modified Eagle's medium (Invitrogen) supplemented with 10% fetal calf serum, 100 μg/ml streptomycin, and 100 units/ml penicillin. Electroporation of cells was performed with a Gene pulser II electroporation system (Bio-Rad) using 4.8×10^6 cells and 10 μg of plasmid DNA. A pSUPER plasmid expressing small interfering RNAs targeting eRF3a mRNA (sh-3a1) has already been described [27]. A pSUPER sh-PAN3 (sh-PAN3) was designed targeting the sequence 5′-GTTA-CATGGTGCCTTCTAG-3′ in human PAN3 mRNA. A pSUPER control directed against 5′-ATTCTCCGAACGTGTCACG-3′ (sh-Ctrl), which has no target in human cells, was used as a negative control. Cells were collected 72 h after electroporation. For some experiments, actinomycin D (5 μg/ml) was added at 72 h and cells collected after 0, 3 or 6 h as indicated in the text [28].
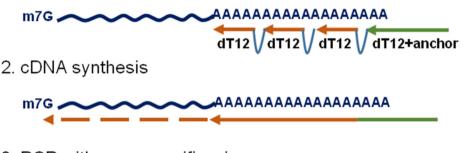
2.2. Western blotting and semi-quantitative RT-PCR

Depletion was ascertained by Western blot analysis or semi-quantitative RT-PCR. 72 h after electroporation with sh-Ctrl, sh-3a1 or sh-PAN3, cells were lysed and Western blotting was performed as already described [29]. Antibodies directed against eRF3a were previously described [27] and antibodies directed against human PAN3 were a generous gift from Dr. Ann-Bin Shyu (University of Texas, Health Science Center, Houston). Antibodies directed against α-tubulin (T6199) were purchased from Sigma. The PAN3 depletion has also been ascertained by semi-quantitative RT-PCR. 72 h after electroporation with sh-Ctrl, sh-3a1 or sh-PAN3, cells were lysed, RNAs were extracted and reverse transcription was achieved with random primer hexamers. 1 μl of template cDNA and 0.5 μM specific primers were used (PAN3 forward primer: 5′AACCTCCAGGCTGAGTAACGTGTC, PAN3 reverse primer: 5′-ATCAGCTCCTGTCGGAGTTCATCA, ACTB forward primer: 5′-TCCCTGGAGAAGAGCTACGA, ACTB reverse primer 5′-AGCACTGTGTTGGCGTACAG) for PCR. ACTB mRNA encoding β-actin was the internal control. 24 amplification cycles were performed for PAN3, and 19 for ACTB. PCR products were analysed by 1.5% agarose gel electrophoresis in the presence of ethidium bromide for UV light transilluminator visualization.

2.3. LM-PAT cDNA synthesis and PAT-PCR analysis

RNA was purified using the NucleoSpin RNA II kit (Macherey-Nagel) according to the manufacturer's instructions and eluted in 40 μl of RNase-free water. LM-PAT experiments were performed according to Sallés et al. [25] with already described modifications [26]. The sequence of the (dT)$_{12}$ - anchor primer was (5′-GCGAGCTCCGCGGCCGCG-T$_{12}$ - 3′). It was used as reverse primer in PCR reactions. PCR forward primers for specific genes (Table 1) were chosen according to the recommendations of Sallés and Strickland [24], i.e., close to the 3′ end of the mRNA body in order to obtain a 250 to 500 base pair long DNA fragment after amplification, which allows a good electrophoretic resolution to be acquired. Standard PCR was performed with GoTaq® G2 Green Master Mix

Fig. 1. Schematic description of the LM-PAT assay: 1. Saturation of the poly(A) tails with oligo(dT)$_{12-18}$ and (dT)$_{12}$ –anchor primer which hybridizes at the 3′-most end of the poly(A) tail followed by ligation. 2. The ligated oligos serve as primer for a cDNA synthesis. 3. cDNA fragments of poly(A) tail are amplified by PCR using a forward gene-specific primer and the (dT)$_{12}$ − anchor primer as reverse primer. PCR forward primers were designed close to the 3′ end of the mRNA in order to obtain 250 to 500 base pairs long DNA fragments after amplification. 4. Poly(A) tail lengths are analysed by agarose gel electrophoresis.

Table 1
Gene specific forward primers used for LM-PAT experiments.

Gene name	Accession Number	Primer (5′ to 3′)	Expected PCR fragment length for minimal poly(A) tail (bp)
ATF4	NM_182810.2	AGGAGGCTCTTACTGGTGAGTGCAA	262
EEF1G	NM_001404.4	TTGCCTTTCCGCTGAGTCCAGATTG	276
RPS6	NM_001010.2	CGTATTGCTCTGAAGAAGCAGCGTA	246
AIMP2	NM_006303.4	GTACTCCAGCAGATCGGAGGCTG	286

(Promega), with 0.5 μM forward gene specific primer, 0.5 μM oligo(dT)-anchor reverse primer and 1 μl of template PAT cDNA in a 25 μl reaction volume. Typically, the PCR conditions were 3 min at 95 °C followed by 25 cycles (for ATF4 and RPS6) or 27 cycles (for EEF1G and AIMP2) of 30 s at 95 °C, 45 s at 60 °C, 1 min at 72 °C, ending with a 7-min final extension at 72 °C. PCR samples were loaded onto a 2% agarose gel in Tris- Borate EDTA buffer and electrophoresis was performed for 3 h at 5 V/cm. After ethidium bromide staining and extensive washing of the gel, photographs were taken using a UV transilluminator Gel Doc XRT (BioRad). The image of the gel was further processed with ImageJ 1.51j8 software. Density profiles were obtained using the Gel Analyzer menu of ImageJ and uncalibrated O.D. option. An area of interest around a first gel lane was designated using the rectangular selection tool and other considered lanes selected in a sequential way. The "plot lanes" option in the gel analyzer menu was used to obtain density profiles for all selected lanes. Peak areas were calculated using the wand tool and, after surface density normalization, gel lane density profiles were superimposed.

3. Results and discussion

3.1. Translation termination factor eRF3a and PAN3 have opposite effect on ATF4 mRNA deadenylation

We first explored the effect of translation termination factor eRF3a and PAN3 subunit of PAN2-PAN3 complex on deadenylation in human cells. In mammals, two distinct eRF3 isoforms, eRF3a and eRF3b, associate with eRF1 to form the translation termination complex and are both able to function as release factors. However, eRF3a is the main factor acting in translation while eRF3b, which is very poorly expressed in most tissues, does not play a major role in translation termination [27,30]. Moreover, we have previously shown that the knockdown of eRF3a also reduced the amount of translation termination factor eRF1, inducing a global defect of translation termination complex [27].

We used plasmids expressing small interfering RNAs directed against either eRF3a (sh-3a1) or PAN3 (sh-PAN3) mRNAs to analyse the effect of eRF3a and PAN3 on poly(A) tail length in the human HCT116 cell line. A plasmid expressing a control shRNA (sh-Ctrl),

which did not target any human mRNAs, was used as a negative control. 72 h after electroporation, the depletion of eRF3a and PAN3 in electroporated cells was ascertained by Western blot and semi-quantitative RT-PCR analyses (see Supplementary Fig. S1) and the poly(A) tail length distribution of various mRNAs were analysed using LM-PAT assays. The choice of the genes to be analysed in LM-PAT assays was dictated by some technical constraints such as the abundance of the mRNAs in the HCT116 cells and the absence of multiple polyadenylation sites that gave complex poly(A) tail profiles. The results of LM-PAT assay for ATF4, EEF1G (eukaryotic elongation factor 1G), RPS6 (ribosomal protein S6), or AIMP2 (aminoacyl tRNA synthetase complex-interacting multifunctional protein 2) are presented in Fig. 2. The same LM-PAT assay was used for all the mRNAs tested, only the gene specific forward primer of the PCR reaction was different. After agarose gel electrophoresis, gel lane profiles were acquired and superimposed after surface density normalization. For each profile, the median length of the poly (A) tail (colored dot lines in the figure) was measured as half of the area covered by the poly (A) tails.

In the steady state conditions presented in Fig. 2, the gel lane profiles allowed to compare the distribution of poly(A) tail lengths in control, eRF3a-depleted and PAN3-depleted cells. For ATF4 mRNA (Fig. 2A), the profiles revealed a global decrease in poly(A) tail length in eRF3a-depleted cells (green line) and a clear increase in PAN3-depleted cells (blue line) when compared to control cells (ochre line). Whereas the median tail length is displaced from ~90 adenosines residues (ochre dotted line) in control HCT116 cells to ~130 adenosines residues (blue dotted line) in PAN3-depleted HCT116 cells, it is decreased from ~90 to ~50 adenosines (green dotted line) in eRF3a-depleted cells (Fig. 2A). Very similar results were obtained in the HEK293 human cell line (Fig. 2A) and with an alternative ATF4 specific primer (data not shown). These results indicate a protective effect of the termination factor eRF3a against ATF4 mRNA deadenylation and show that the deadenylation is initiated by the PAN2-PAN3 complex. The opposite effect of eRF3a and PAN3 knockdowns on poly(A) tail length are coherent with the predicted competitive binding between eRF3 and deadenylation complexes on PABP [10]. These findings strongly suggest that ATF4 mRNA poly(A) tail is subject to a biphasic deadenylation process [5].

However, in our hands, ATF4 mRNA remained an exception among the mRNAs tested. Indeed, the depletion of either eRF3a or PAN3 had only a very weak, if not absent, effect on the poly (A) tail length distribution for the other genes studied (Fig. 2B). This result could be indicative that these mRNAs experienced another degradation process than the biphasic process initiated by PAN2-PAN3 complex, possibly a single step deadenylation process. It has been already suggested that the sequential model for deadenylation is an oversimplification [31]. The factors and circumstances that determine the choice of either PAN2-PAN3 or CCR4-NOT complex at the initiation of deadenylation remain obscure. PAN2-PAN3 and CCR4—NOT complexes could differ in substrate preference and thus target different mRNA populations for degradation [31,32].

While it is now established that PAN2-PAN3 has a clear preference for longer poly(A) tail and the CCR4-NOT complex for shorter poly(A) tails, the basis for these substrate preferences are unknown [7]. The median poly(A) tail length is about 90 adenosine residues in the case of ATF4 mRNA, and 50 for EEF1G, RPS6 and AIMP2 (Fig. 2). The slight effect of PAN3 depletion on poly(A) tail length for EEF1G and RPS6 mRNAs could nevertheless be indicative of PAN2-PAN3 complex involvement in their deadenylation. In this case, the timing of the transition from the initial phase of deadenylation performed by PAN2-PAN3 to the second phase involving CCR4-NOT complex (a rapid transition for EEF1G, RPS6 and AIMP2 and a much slower transition for ATF4) could explain the difference between ATF4 and the other genes tested.

3.2. Biphasic deadenylation of ATF4 mRNA

In the above experiments, we observed poly (A) tail lengths which are determined by the balance between transcription and degradation of mRNA, i.e. in steady-state conditions. However, degradation of the poly (A) tail is a post-transcriptional event which is primarily cytoplasmic. Thus, to observe the tail length dynamics of endogenous mRNAs, we thought to measure poly (A) tail length changes after inhibition of transcription, i.e., when the changes are assumed to reflect degradation only. For this purpose, 72 h after cell electroporation with sh-Ctrl, sh-3a1 or sh-PAN3, the transcriptional inhibitor actinomycin D (ActD) was added into cell culture medium for 0, 3 or 6 h. For each time point, the poly(A) tail length distribution of ATF4, AIMP2, EEF1G and RPS6 mRNAs were analysed in eRF3a-depleted, PAN3-depleted and control cells using LM-PAT assays. After agarose gel electrophoresis, lane profiles were acquired and profiles of eRF3a knockdown, PAN3 knockdown and control cells were superimposed for the different times of Actinomycin D (Fig. 3 and Supplemental Figs. S2 and S3). As expected, the tail lengths of each mRNA tested gradually decreased after inhibition of transcription, with median tail lengths shortening to about half of their original length over the course of the experiment (e. g., the median tail length decreased to ~50 nucleotides for ATF4 in Fig. 3A, ochre dotted line). The global tail length reduction in the absence of newly synthesized mRNAs is indicative of the ongoing deadenylation process.

For ATF4 mRNA, actinomycin D treatment highlighted the impact of PAN3 depletion, revealing a progressive decrease in the longest poly(A) tail over the time of the experiment (blue lines on Fig. 3A). At 6 h time point, the curves of control (ochre line) and PAN3-depleted cells (blue line) are overlapping, suggesting that the PAN2-PAN3 deadenylation phase ended. Besides, the decrease in the poly (A) tail length in eRF3a depleted cells remains visible up to 6 h of ActD treatment (green lines on Fig. 3A), and demonstrates that the protective effect of eRF3a against poly (A) tail deadenylation is still effective despite the overall tail length reduction. In the case of EEF1G, RPS6 (Fig. 3B) and AIMP2 (Supplemental Fig. S2), the superimposition of the density profiles at 0 h and 6 h does not allow to assume influence of either eRF3a or PAN3 on deadenylation kinetics. Only the global poly(A) tail length decrease with time is observable.

The preferential protection of long-tailed ATF4 molecules in PAN3-depleted cells favored the view that deadenylation of ATF4 mRNA is initiated by the PAN2-PAN3 complex. The accumulation of short poly(A)-tailed mRNA molecules at the expense of the longer ones after 6 h of ActD treatment could testify to the switch to the second degradation phase performed by the CCR4-NOT complex once the first deadenylation step is completed. This reinforces the idea that the deadenylation of ATF4 mRNA obeys the two-phase model.

For the other mRNA species tested that do not appear to follow this two-phase process, a one-step process involving the CCR4-NOT complex can be postulated. However, there are some arguments that could support the idea that the biphasic deadenylation model is also applicable to these mRNAs. A strong argument is given by the fact that there is evidence that the PAN2-PAN3 and CCR4-NOT complexes interact in larger assembly including PABP [33]. Thus, a unique deadenylation machinery would be responsible for poly(A) tail degradation whatever the mRNA concerned and whatever the initial length of its poly(A) tail. Moreover, the sequential action of PAN2-PAN3 and CCR4—NOT was deduced from in vivo [5] and in vitro [7] experiments showing that the two deadenylase complexes have different substrate preferences. In an in vitro system [7], PAN2-PAN3 can effectively degrade a poly(A) tail long enough to span three poly(A)-bound PABP. Deadenylation
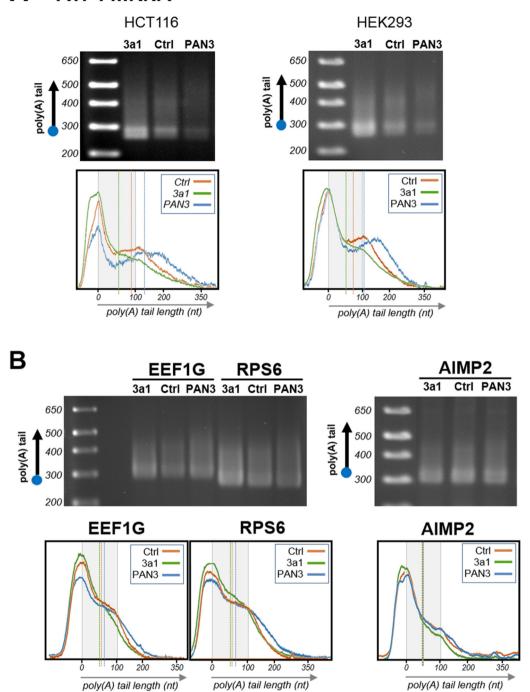
Fig. 2. Distribution of ATF4, EEF1G, RPS6 and AIMP2 poly(A) tail length in steady state conditions, after eRF3a or PAN3 depletion. Three days after cell electroporation with a control plasmid (Ctrl) or plasmids expressing small interfering RNAs targeting eRF3a mRNA (3a1) or PAN3 mRNA (PAN3), RNAs were extracted and subjected to LM-PAT assay. For each LM-PAT reaction, after cDNA synthesis, DNA fragments were amplified with forward primers specific for ATF4 (**A**), EEF1G, RPS6 and AIMP2 (**B**).The agarose gel of PCR reactions is shown at the top. The first lane corresponds to DNA ladder (in base pair on the left). Below the gel, the superimposition of the gel lane profiles of control cells (ochre line), eRF3a-depleted cells (green line) and PAN3-depleted cells (blue line) is shown. In each case, the dotted line indicates the median poly(A) tail length. The grey window underlines the accumulation of products with 100 adenosine tails. Electroporation of HCT116 and HEK293 cell lines are presented for ATF4 (**A**), while only HCT116 cells are displayed for EEF1G, RPS6 and AIMP2 (**B**).

by PAN2-PAN3 is less active on a shorter tail spanning only two PABP molecules and is ineffective when the poly(A) tail has been shortened to span a single PABP [7]. These in vitro experiments suggest that the transfer of the deadenylation process to CCR4-NOT complex usually occurs when the poly(A) tail has been shortened to

contain only two PABPs. This model fits well with yeast transcripts for which the initial length of the poly(A) tail is limited to around 90 nucleotides with a median tail length of about 30 adenosines [7,34]. However, in mammalian cells it has been observed that CCR4-NOT complex is active on longer poly(A) tails ranging up to 100
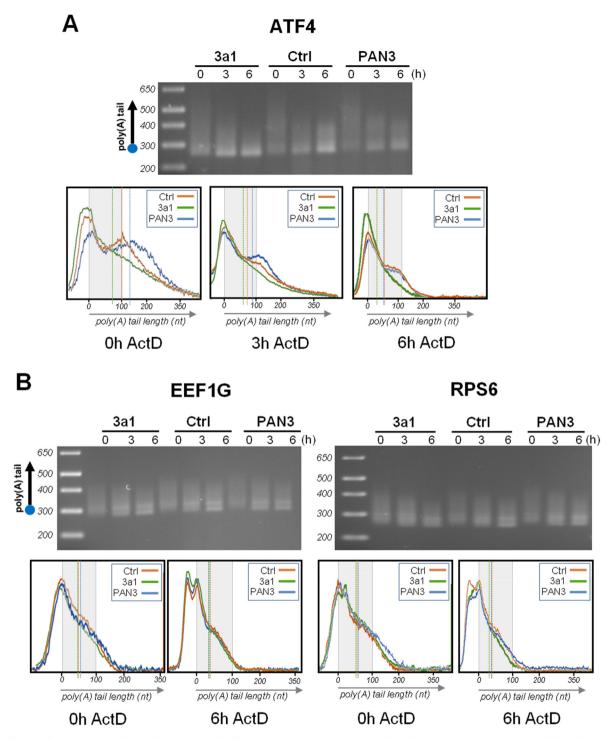
Fig. 3. Distribution of ATF4, EEF1G and RPS6 poly(A) tail lengths after actinomycin D treatment. Three days after electroporation with a control plasmid (Ctrl), or plasmids expressing small interfering RNAs targeting eRF3a mRNA (3a1) or PAN3 mRNA (PAN3), HCT116 cells were treated with actinomycin D for 0, 3 and 6 h as indicated above the gel panel. RNAs were extracted and subjected to LM-PAT analysis. For each LM-PAT reaction, after cDNA synthesis, DNA fragments were amplified with forward primers specific for ATF4 (**A**), EEF1G and RPS6 (**B**). The agarose gel of PCR reactions is shown at the top. The first lane corresponds to DNA ladder (in base pair on the left). Below the gel, the superimposition of the gel lane profiles of control cells (ochre line), eRF3a-depleted cells (green line) and PAN3-depleted cells (blue line) is shown at 0, 3 and 6 h of actinomycin D treatment for ATF4 (**A**) and 0 and 6 h for EEF1G and RPS6 (**B**). In each case, the dotted line indicates the median poly(A) tail length. The grey window underlines the accumulation of products with 100 adenosine tails.

adenosine residues [5,10]. Thus, it is quite possible, that for mRNAs with median tail length just over 50 adenosines, such as EEF1G, RPS6 and AIMP2 (Fig. 2), the initial PAN2-PAN3 deadenylation phase is greatly reduced by a rapid switch to the CCR4-NOT phase.

The differences in the timing of the transition from one phase to the other could explain the difficulties encountered in the generalization of the biphasic deadenylation model.

3.3. Conclusion

The above experiments show that the deadenylation of endogenous ATF4 mRNA is in accordance with the biphasic mechanism model [5,11] and is also consistent with the predicted competitive binding of eRF3 and deadenylation complexes on PABP [10]. This raises the evidence that biphasic deadenylation of mRNAs occurs in human cells. However, further experiments are needed to establish whether this mechanism is generalizable.

Author contributions

BJ and OJ-J conceived and designed the project, BJ acquired the data, BJ and OJ-J analysed and interpreted the data, BJ and OJ-J wrote the paper.

Declaration of competing interest

I have no conflict of interest.

Acknowledgements

Appendix A. Supplementary data

Supplementary data to this article can be found online at https://doi.org/10.1016/j.biochi.2021.03.013.

References

[1] A.B. Shyu, J.G. Belasco, M.E. Greenberg, Two distinct destabilizing elements in the c-fos message trigger deadenylation as a first step in rapid mRNA decay, Genes Dev. 5 (1991) 221–231.

[2] D.T. Fritz, N. Bergman, W.J. Kilpatrick, C.J. Wilusz, J. Wilusz, Messenger RNA decay in mammalian cells: the exonuclease perspective, Cell Biochem. Biophys. 41 (2004) 265–278, https://doi.org/10.1385/CBB:41:2:265.

[3] R. Parker, H. Song, The enzymes and control of eukaryotic mRNA turnover, Nat. Struct. Mol. Biol. 11 (2004) 121–127, https://doi.org/10.1038/nsmb724.

[4] E. Wahle, G.S. Winkler, RNA decay machines: deadenylation by the Ccr4-not and Pan2-Pan3 complexes, Biochim. Biophys. Acta 1829 (2013) 561–570, https://doi.org/10.1016/j.bbagrm.2013.01.003.

[5] A. Yamashita, T.-C. Chang, Y. Yamashita, W. Zhu, Z. Zhong, C.-Y.A. Chen, A.-B. Shyu, Concerted action of poly(A) nucleases and decapping enzyme in mammalian mRNA turnover, Nat. Struct. Mol. Biol. 12 (2005) 1054–1063, https://doi.org/10.1038/nsmb1016.

[6] N. Uchida, S.-I. Hoshino, H. Imataka, N. Sonenberg, T. Katada, A novel role of the mammalian GSPT/eRF3 associating with poly(A)-binding protein in Cap/Poly(A)-dependent translation, J. Biol. Chem. 277 (2002) 50286–50292, https://doi.org/10.1074/jbc.M203029200.

[7] I.B. Schäfer, M. Yamashita, J.M. Schuller, S. Schüssler, P. Reichelt, M. Strauss, E. Conti, Molecular basis for poly(A) RNP architecture and recognition by the Pan2-Pan3 deadenylase, Cell 177 (2019) 1619–1631, https://doi.org/10.1016/j.cell.2019.04.013.

[8] M. Tucker, M.A. Valencia-Sanchez, R.R. Staples, J. Chen, C.L. Denis, R. Parker, The transcription factor associated Ccr4 and Caf1 proteins are components of the major cytoplasmic mRNA deadenylase in Saccharomyces cerevisiae, Cell 104 (2001) 377–386, https://doi.org/10.1016/s0092-8674(01)00225-2.

[9] M. Bartlam, T. Yamamoto, The structural basis for deadenylation by the CCR4-NOT complex, Protein Cell 1 (2010) 443–452, https://doi.org/10.1007/s13238-010-0060-8.

[10] Y. Funakoshi, Y. Doi, N. Hosoda, N. Uchida, M. Osawa, I. Shimada, M. Tsujimoto, T. Suzuki, T. Katada, S. Hoshino, Mechanism of mRNA deadenylation: evidence for a molecular interplay between translation termination factor eRF3 and mRNA deadenylases, Genes Dev. 21 (2007) 3135–3148, https://doi.org/10.1101/gad.1597707.

[11] N. Ezzeddine, T.-C. Chang, W. Zhu, A. Yamashita, C.-Y.A. Chen, Z. Zhong, Y. Yamashita, D. Zheng, A.-B. Shyu, Human TOB, an antiproliferative transcription factor, is a poly(A)-binding protein-dependent positive regulator of cytoplasmic mRNA deadenylation, Mol. Cell Biol. 27 (2007) 7791–7801, https://doi.org/10.1128/MCB.01254-07.

[12] P. Bernstein, S.W. Peltz, J. Ross, The poly(A)-poly(A)-binding protein complex is a major determinant of mRNA stability in vitro, Mol. Cell Biol. 9 (1989) 659–670.

[13] N. Siddiqui, D.A. Mangus, T.-C. Chang, J.-M. Palermino, A.-B. Shyu, K. Gehring, Poly(A) nuclease interacts with the C-terminal domain of polyadenylate-binding protein domain from poly(A)-binding protein, J. Biol. Chem. 282 (2007) 25067–25075, https://doi.org/10.1074/jbc.M701256200.

[14] M. Osawa, N. Hosoda, T. Nakanishi, N. Uchida, T. Kimura, S. Imai, A. Machiyama, T. Katada, S. Hoshino, I. Shimada, Biological role of the two overlapping poly(A)-binding protein interacting motifs 2 (PAM2) of eukaryotic releasing factor eRF3 in mRNA decay, RNA 18 (2012) 1957–1967, https://doi.org/10.1261/rna.035311.112.

[15] C.Y. Chen, A.B. Shyu, AU-rich elements: characterization and importance in mRNA degradation, Trends Biochem. Sci. 20 (1995) 465–470, https://doi.org/10.1016/s0968-0004(00)89102-1.

[16] I. Legnini, J. Alles, N. Karaiskos, S. Ayoub, N. Rajewsky, FLAM-seq: full-length mRNA sequencing reveals principles of poly(A) tail length control, Nat. Methods 16 (2019) 879–886, https://doi.org/10.1038/s41592-019-0503-y.

[17] A.O. Subtelny, S.W. Eichhorn, G.R. Chen, H. Sive, D.P. Bartel, Poly(A)-tail profiling reveals an embryonic switch in translational control, Nature 508 (2014) 66–71, https://doi.org/10.1038/nature13007.

[18] H. Chang, J. Lim, M. Ha, V.N. Kim, TAIL-seq: genome-wide determination of poly(A) tail length and 3' end modifications, Mol. Cell. 53 (2014) 1044–1052, https://doi.org/10.1016/j.molcel.2014.02.007.

[19] T.J. Eisen, S.W. Eichhorn, A.O. Subtelny, K.S. Lin, S.E. McGeary, S. Gupta, D.P. Bartel, The dynamics of cytoplasmic mRNA metabolism, Mol. Cell. 77 (2020) 786–799, https://doi.org/10.1016/j.molcel.2019.12.005.

[20] F. Yu, Y. Zhang, C. Cheng, W. Wang, Z. Zhou, W. Rang, H. Yu, Y. Wei, Q. Wu, Y. Zhang, Poly(A)-seq: a method for direct sequencing and analysis of the transcriptomic poly(A)-tails, PloS One 15 (2020), https://doi.org/10.1371/journal.pone.0234696 e0234696.

[21] A. Łabno, R. Tomecki, A. Dziembowski, Cytoplasmic RNA decay pathways - enzymes and mechanisms, Biochim. Biophys. Acta 1863 (2016) 3125–3147, https://doi.org/10.1016/j.bbamcr.2016.09.023.

[22] T.T.L. Tang, J.A.W. Stowell, C.H. Hill, L.A. Passmore, The intrinsic structure of poly(A) RNA determines the specificity of Pan2 and Caf1 deadenylases, Nat. Struct. Mol. Biol. 26 (2019) 433–442, https://doi.org/10.1038/s41594-019-0227-9.

[23] A.L. Nicholson, A.E. Pasquinelli, Tales of detailed poly(A) tails, Trends Cell Biol. 29 (2019) 191–200, https://doi.org/10.1016/j.tcb.2018.11.002.

[24] F.J. Sallés, S. Strickland, Rapid and sensitive analysis of mRNA polyadenylation states by PCR, PCR Methods Appl. 4 (1995) 317–321.

[25] F.J. Sallés, W.G. Richards, S. Strickland, Assaying the polyadenylation state of mRNAs, Methods San Diego Calif 17 (1999) 38–45, https://doi.org/10.1006/meth.1998.0705.

[26] B. Jolles, A. Aliouat, V. Stierlé, S. Salhi, O. Jean-Jean, Translation termination-dependent deadenylation of MYC mRNA in human cells, Oncotarget 9 (2018) 26171–26182, https://doi.org/10.18632/oncotarget.25459.

[27] C. Chauvin, S. Salhi, C. Le Goff, W. Viranaicken, D. Diop, O. Jean-Jean, Involvement of human release factors eRF3a and eRF3b in translation termination and regulation of the termination complex formation, Mol. Cell Biol. 25 (2005) 5801–5811, https://doi.org/10.1128/MCB.25.14.5801-5811.2005.

[28] D. Kögel, R. Schomburg, T. Schürmann, H.-G. König, M. Poppe, A. Eckert, W.E. Müller, J.H.M. Prehn, The amyloid precursor protein protects PC12 cells against endoplasmic reticulum stress-induced apoptosis, J. Neurochem. 87 (2003) 248–256, https://doi.org/10.1046/j.1471-4159.2003.02000.x.

[29] H. Ait Ghezala, B. Jolles, S. Salhi, K. Castrillo, W. Carpentier, N. Cagnard, A. Bruhat, P. Fafournoux, O. Jean-Jean, Translation termination efficiency modulates ATF4 response by regulating ATF4 mRNA translation at 5' short ORFs, Nucleic Acids Res. 40 (2012) 9557–9570, https://doi.org/10.1093/nar/gks762.

[30] S. Hoshino, M. Imai, M. Mizutani, Y. Kikuchi, F. Hanaoka, M. Ui, T. Katada, Molecular cloning of a novel member of the eukaryotic polypeptide chain-releasing factors (eRF). Its identification as eRF3 interacting with eRF1, J. Biol. Chem. 273 (1998) 22254–22259, https://doi.org/10.1074/jbc.273.35.22254.

[31] J.S. Mugridge, J. Coller, J.D. Gross, Structural and molecular mechanisms for the control of eukaryotic 5'-3' mRNA decay, Nat. Struct. Mol. Biol. 25 (2018) 1077–1085, https://doi.org/10.1038/s41594-018-0164-z.

[32] M. Sun, B. Schwalb, N. Pirkl, K.C. Maier, A. Schenk, H. Failmezger, A. Tresch, P. Cramer, Global analysis of eukaryotic mRNA degradation reveals Xrn1-dependent buffering of transcript levels, Mol. Cell. 52 (2013) 52–62, https://doi.org/10.1016/j.molcel.2013.09.010.

[33] D. Zheng, N. Ezzeddine, C.-Y.A. Chen, W. Zhu, X. He, A.-B. Shyu, Deadenylation is prerequisite for P-body formation and mRNA decay in mammalian cells, J. Cell Biol. 182 (2008) 89–101, https://doi.org/10.1083/jcb.200801196.

[34] C.E. Brown, A.B. Sachs, Poly(A) tail length control in Saccharomyces cerevisiae occurs by message-specific deadenylation, Mol. Cell Biol. 18 (1998) 6548–6559, https://doi.org/10.1128/mcb.18.11.6548.